Uncoordinated Transmissions in Uplink IoT Cell-Free Massive MIMO Systems based on NOMA

Joumana Farah, Cybele Ghanem, Eric Pierre Simon

Uncoordinated Transmissions in Uplink IoT Cell-Free Massive MIMO Systems based on NOMA

Joumana Farah*, Cybele Ghanem†, Eric Pierre Simon‡
*Univ Rennes, INSA Rennes, CNRS, IETR-UMR 6164, F-35000 Rennes, France
†Faculty of Engineering, Lebanese University, Roumieh, Lebanon
‡University of Lille, CNRS, UMR 8520 - IEMN Lille

***Abstract*—This paper presents a new framework comprising the combination of uplink cell-free massive multiple input multiple output (mMIMO) with non-orthogonal multiple access (NOMA) for serving Internet-of-Things (IoT) devices in an uncoordinated manner. We investigate the benefits of reinforcement learning to support the massive connectivity and quality of service (QoS) requirements of IoT devices. Using the multi-armed bandit technique, the devices jointly determine their subband and transmit power, without any cooperation, in such a way as to strike a balance between the QoS and the transmit power. Applied with a dynamic cooperation clustering of serving access points (APs), the allocation technique is shown to achieve a quick convergence while having a negligible loss in performance towards a system that relies on all deployed APs for serving the devices.**

***Index Terms*—IoT, NOMA, Cell-free networks, massive MIMO, channel allocation, power control, uncoordinated transmissions.**

I. Introduction

During the last decade, Internet-Of-Things (IoT) communications have witnessed massive growth due to the generalization of various applications related to connected healthcare, autonomous vehicles, industrial automation, and environmental monitoring, among others. These spreading applications open the door to new challenges and constraints that researchers and engineers must face to cope with the limited spectrum and high interference generated by massive connectivity. In particular, 5G and beyond standards are urged to design a reliable communication framework with low latency and minimum complexity features. In order to fulfill these requirements, new network schemes need to be introduced. In fact, traditional cellular networks currently deployed have so far failed to ensure an acceptable level of uniformity in the quality of service (QoS) offered to users or devices. Instead, large variations of data rates are witnessed throughout the cells, with high peaks at cell centers and a low QoS at cell-edges. An alternative structure has recently emerged, namely, cell-free massive multiple input multiple output (CF-mMIMO) [1], [2], where an important number of access points (APs) are distributed over the deployment area and cooperate to serve cellular users or IoT devices optimally. Each of these densely deployed APs is equipped with a small number of antennas and is connected to a central processing unit (CPU) via fronthaul links constituted by high-capacity coaxial cables or fiber optics. Indeed, the uniformity of the signal quality in the cell-free context was proven in [3], [4], [5], [6] through practical channel measurements.

Several previous works dealt with resource allocation in the context of uplink CF-mMIMO. In [7], deep reinforcement learning and sequential convex approximation (SCA) are used to solve the sum-rate fairness trade-off power optimization problem. The work in [8] proposes low-complexity solutions based on deep learning for solving the max-min, max-product, and max-sum-rate power control problems. The joint optimization of receive combining and power control is performed in [9] using a mirror prox-based method. Low-complexity convex algorithms are used in [10] for joint power control and AP scheduling under stringent fronthaul bandwidth constraints.

Another promising paradigm that is envisioned as an efficient lever for cell-free networks is that of non-orthogonal multiple access (NOMA). The importance of combining NOMA with cell-free architectures is stressed in [11] for properly handling interference in massive IoT transmissions. However, most of the works on resource allocation in CF-mMIMO-NOMA focus on downlink transmissions, while only a few consider the uplink context. In [12], the power allocation problem is solved by SCA to maximize the total spectral efficiency in CF-mMIMO-NOMA while respecting quality-of-service (QoS), transmit power, and successive interference cancellation (SIC) constraints. Optimal combining is considered in [13] with max-min QoS power control and user grouping. Optimal power control is also studied in [14], [15]. While all these works show the importance of combining NOMA with CF-mMIMO in uplink transmissions, none of them considers subband or channel allocation.

In this work, we focus on uncoordinated power control and spectrum access which has recently received a rising interest from the research community [16], [17], [18]. In such systems, users choose their channel and transmit data whenever needed without having to formulate a prior scheduling request to the control unit. Such distributed strategies greatly reduce communication latency and signaling overhead. However, the problem of collisions that arises in this framework needs to be addressed by proper multiple access techniques, leveraging NOMA and/or reinforcement learning techniques that allow devices to adjust their transmissions and minimize collisions distributively [18], [19]. To our knowledge, this is the first work considering uncoordinated uplink transmissions in CF-mMIMO-NOMA. We develop a solution to the joint subband

and power allocation based on the multi-player multi-armed bandit (MAB) framework [20], [17], [18] with zero-reward on collision. We particularly show how the MAB algorithm can be adapted to the special context of CF-mMIMO-NOMA. For this purpose, in section II, we start by detailing the system model. Then, section III shows the adaptation of the Upper Confidence Bound (UCB) algorithm from [19] to CF-mMIMO-NOMA. Section IV summarizes the simulation results and analyses, while section V concludes the paper.

II. System Model

The communication network comprises L APs randomly deployed over a large coverage area, with N antennas per AP. K single-antenna devices transmit signals on C available subbands and are jointly received by the APs. These K devices are an active subset from a larger set of randomly deployed IoT devices that transmit information when needed. We denote by $\mathbf{h}_{k,l,c}$ the $N \times 1$ channel vector between device k and AP l on subband c, each element containing the channel amplitude between k and one of the N antennas of l on this specific subband. The channel amplitudes follow the random model in [21] which includes correlated Rayleigh fading, path loss and shadowing. The devices are supposed to be stationary during the transmission phase. All APs receive a superposition of the signals sent from all devices. The received signal at AP l on subband c is:

$$\mathbf{y}_{l,c} = \sum_{k=1}^{K} \mathbf{h}_{k,l,c} s_{k,c} + \mathbf{n}_{l,c}, \tag{1}$$

where $s_{k,c}$ is the signal transmitted from device k on subband c with a power $p_{k,c}$ and $\mathbf{n}_{l,c}$ is the complex additive Gaussian noise, $\mathbf{n}_{l,c} \sim \mathcal{N}(\mathbf{0}_N, \sigma^2 \mathbf{I}_N)$. Each device has a maximum power budget $p^{\max}$ that it must not exceed and sends its information on a unique subband.

The dynamic cooperation clustering (DCC) framework from [21] is adopted with the AP selection technique from [22] being applied prior to the communication phase to determine the subset of APs that serve each device k. Let $\mathcal{M}_k \subset \{1, 2, \ldots, L\}$ be the subset of indices of the APs serving k. Also, define the $N \times N$ matrix $\mathbf{D}_{k,l}$ which equals the identity matrix $\mathbf{I}_N$ if k is served by AP l or $\mathbf{0}_{N \times N}$ otherwise. The channel amplitudes are assumed to be perfectly known by the devices through proper channel estimation techniques which are beyond the scope of this paper. This knowledge is needed for the uncoordinated setup, where devices access channels without the need to be granted access beforehand by the CPU. In this work, we mainly focus on the centralized operation of the network, where APs act as remote radio heads (RRHs) as in [23], [24]. However, the distributed operation [21] can be applied as an extension to this study. In uplink, the APs forward their received signals to the CPU through the fronthaul links that are assumed to be error-free. The CPU performs receive combining on the received signals, yielding the estimate of the symbol of user k on subband c:

$$\hat{s}_{k,c} = \mathbf{v}_{k,c}^H \mathbf{D}_k \mathbf{y}_c, \tag{2}$$

where $\mathbf{y}_c = [\mathbf{y}_{1,c}^T, \cdots, \mathbf{y}_{L,c}^T]^T$ is the collective received signal, $\mathbf{D}_k = \mathrm{diag}(\mathbf{D}_{k,1}, \mathbf{D}_{k,2}, \cdots, \mathbf{D}_{k,L})$ a $M \times M$ block diagonal matrix ($M = N \times L$) and $\mathbf{v}_{k,c}$ the receive combining vector for the signal of k on c. Assuming perfect channel estimation at the CPU, the signal-to-interference ratio (SINR) for the signal of user k is given by:

$$\Gamma_k = \frac{p_{k,c} |\mathbf{v}_{k,c}^H \mathbf{D}_k \mathbf{h}_{k,c}|^2}{\sum_{k'=1, k' \neq k}^{K} p_{k',c} |\mathbf{v}_{k,c}^H \mathbf{D}_k \mathbf{h}_{k',c}|^2 + \sigma^2 \|\mathbf{D}_k \mathbf{v}_{k,c}\|^2}, \tag{3}$$

where $\mathbf{h}_{k,c}$ is the $M \times 1$ collective channel of k: $\mathbf{h}_{k,c} = [\mathbf{h}_{k,1,c}^H, \mathbf{h}_{k,2,c}^H, \cdots, \mathbf{h}_{k,L,c}^H]^H$. Note that (3) will subsequently be modified to take into account the specific SIC scheme and power control in NOMA. Moreover, the time index, corresponding to a particular timeslot t, has not been added to powers, channels, and combining vectors to simplify notations.

In this work, channel assignment and power control are jointly determined using an uncoordinated spectrum access technique that does not require any communication between devices nor a centralized allocation by the CPU. More specifically, we rely on NOMA and generalize the power control model in [25], [19] to the cell-free context. Its aim is to enable multiple devices to transmit on the same subband while achieving a non-zero rate. This is done by ensuring that the received power levels of the devices sharing a subband are distinct enough to enable SIC decoding at the CPU. Let J be the number of available received power levels per subband and Γ^r the required SINR to guarantee a corresponding requested QoS for each device. It can be shown [25] that the j^{th} received power level $q_j, j = 1, \cdots, J$ ($q_1 > q_2 > \ldots > q_J$), to guarantee the required SINR, is:

$$q_j = \sigma^2 \Gamma^r (\Gamma^r + 1)^{J-j}. \tag{4}$$

To reach a received power level q_j on a subband c, each device k evaluates its needed transmit power according to:

$$p_{k,c} = \frac{q_j}{|\mathbf{v}_{k,c}^H \mathbf{D}_k \mathbf{h}_{k,c}|^2}. \tag{5}$$

For the signals to be successfully decoded at the CPU, the number of devices transmitting on each subband must not exceed that of the power levels J, and devices must select different power levels. Otherwise, power collisions occur. Since SIC in uplink NOMA is done in the descending order of the received power levels, when a collision takes place on a specific power level j, all signals received on levels $i, i \geq j$, are lost and cannot be recovered. Moreover, the collision can also cause upper-level signals to be undecodable if their target SINR is not reached.

Several receive combining techniques can be used in uplink CF-mMIMO [21], like the optimum minimum mean squared error (MMSE) or the more scalable maximal ratio (MR) combining scheme. The first is given by:

$$\mathbf{v}_{k,c} = p_{k,c} \left(\sum_{k'=1}^{K} p_{k',c} \mathbf{D}_k \mathbf{h}_{k',c} \mathbf{h}_{k',c}^H \mathbf{D}_k + \sigma^2 \mathbf{I}_M \right)^{-1} \mathbf{D}_k \mathbf{h}_{k,c}, \tag{6}$$

whereas the MR combining vector is $\mathbf{v}_{k,c} = \mathbf{D}_k \mathbf{h}_{k,c}$. In order to determine its transmit power on subband c and power level j using (5), device k needs to evaluate the detection vector that will be applied at the CPU level. Since the MMSE combining involves transmit powers and channel gains of other devices for proper inter-user interference cancelation, and since such information cannot be available at device k, (6) cannot be used to find $\mathbf{v}_{k,c}$. Moreover, applying (6) at the CPU for receive combining requires that the latter have an exact knowledge of all the device's transmit powers, which is not in the spirit of uncoordinated communications. Therefore, we propose to rely instead on the MR combining since, in addition to being less complex to implement compared to MMSE, it only involves the channel gain of k.

III. Description of the uncoordinated resource allocation strategy

The multi-player MAB framework with zero-reward on collision [20], [17], [18] is used to model the joint subband allocation and power control problem. In this framework, each player (*i.e.* device) k first builds its action profile $\mathcal{A}_k$ from its available set of arms, as was done in [19]. $\mathcal{A}_k$ is constituted by the subband-power level pairs on which the device can transmit without violating its power budget $p^{\max}$: $\mathcal{A}_k$=$\{a_1, a_2, \ldots, a_{M_k}\}$, where M_k is the number of valid arms for k. Upon choosing an action a_m, each device k receives a reward from the CPU given by the following utility function:

$$U_{k,a_m} = \eta_{k,a_m} \times B_c \log_2(1 + \Gamma_{k,a_m}). \tag{7}$$

In (7), η_{k,a_m} is the collision indicator for k on arm a_m, which is zero in case of a power collision (*i.e.* 2 or more users choosing the same power level on a subband or when $\Gamma_{k,a_m} < \Gamma^r$), and 1 otherwise. B_c is the subband bandwidth and Γ_{k,a_m} the achieved SINR of device k when choosing action a_m, given by:

$$\Gamma_{k,a_m} = \frac{q_i}{\sum_{l \in \mathcal{B}_{i,c}} p_{l,c} |\mathbf{v}_{k,c}^H \mathbf{D}_k \mathbf{h}_{l,c}|^2 + \sigma^2 \|\mathbf{D}_k \mathbf{v}_{k,c}\|^2}, \tag{8}$$

where q_i is the power level chosen in action a_m by device k and $\mathcal{B}_{i,c}$ is the index set of users having chosen the subband c and received power level $q_j, j > i$. The sum in the denominator of (8) accounts for the interference of the other devices signals that have not yet been canceled with SIC, while decoding the signal of k.

The uncoordinated resource allocation problem in the CF-mMIMO-NOMA context is solved by using the UCB algorithm proposed in [26] as well as its enhanced version from [19]. The latter extends the UCB technique in such a way as to consider the power consumption of the devices to optimize their battery life. To this aim, the best arm identification is modified in the enhanced UCB algorithm to balance the achieved rate on the considered arm and the necessary transmit power. Therefore, device k selects its best arm based on:

$$a_{\text{best}}^{(k)} = \underset{a_m \in \mathcal{A}_k}{\arg\max} \left(\alpha \frac{\log_2(1 + \Gamma_{k,a_m})}{\log_2(1 + \frac{q_1}{\sigma^2})} - \beta \frac{p_{k,c}}{p^{\max}} \right), \tag{9}$$

where α and β are two positive weights s.t. $\alpha + \beta = 1$. Note that each term in (9) has been normalized by its maximum possible value, and $p_{k,c}$ is estimated by device k using (5) for arm m. The uncoordinated joint channel and power allocation technique is summarized in Algorithm 1, where T is the time horizon, t the timeslot index, and $n_k(a_i, t)$ the number of times arm a_i is played by device k until timeslot t.

Algorithm 1: Enhanced UCB allocation

Initialization: Each device k explores the actions in $\mathcal{A}_k$ by playing the arms in random order and collecting their utilities.
for *t=1:T* **do**
  for *k=1:K* **do**
    // k identifies its best arm:
    $a_{\text{best}}^{(k)} = \underset{a_m \in \mathcal{A}_k}{\arg\max} \left(\alpha \frac{Q(k,a_m) + \sqrt{\frac{2\log(t)}{n_k(a_m,t)}}}{B_c \log_2(1+\frac{q_1}{\sigma^2})} - \beta \frac{p_{k,c}}{p^{\max}} \right)$
    //k updates its parameters based on its received utility:
    $s_k(a_{\text{best}}^{(k)}, t+1) = s_k(a_{\text{best}}^{(k)}, t) + U_{k,a_{\text{best}}^{(k)}}$
    $n_k(a_{\text{best}}^{(k)}, t+1) = n_k(a_{\text{best}}^{(k)}, t) + 1$
    $Q(k, a_{\text{best}}^{(k)}) = \frac{s_k(a_{\text{best}}^{(k)}, t+1)}{n_k(a_{\text{best}}^{(k)}, t+1)}$
  end
end

IV. Simulation results and discussions

In the simulation setup of the CF-mMIMO-NOMA system, a coverage area of 1 Km × 1 Km is considered with a wrap-around topology [21]. $L = 100$ APs are randomly deployed over the area, and each one is equipped with a half-wavelength-spaced uniform linear array of $N = 4$ antennas. $K = 50$ users are served over $C = 10$ subbands of bandwidth $B_c = 180$ kHz, equivalent to the bandwidth of a resource block in 5G networks. $J = 5$ power levels are considered per subband. The power budget $p^{\max}$ is set to 23 dBm. The APs noise power is -114 dBm, with a noise factor of 7 dB. Algorithm 1 (indicated by "Enhanced-UCB") is applied with $\alpha = \beta = 0.5$ and a time horizon of $T = 200$ timeslots of 1 ms each. Its performance is analyzed for the DCC setup as well as another one, indicated by "ALL" in the graphs, where all L APs jointly serve the K users (*i.e.* no AP selection is applied). Also, the performance of two other allocation techniques are shown for comparison in both DCC and ALL setups: the random subband and power level access (indicated by "RA") and the basic UCB algorithm (indicated by "UCB") from [26]. The latter uses $a_{\text{best}}^{(k)} = \underset{a_m \in \mathcal{A}_k}{\arg\max} \left(Q(k, a_m) + \sqrt{\frac{2\log(t)}{n_k(a_m,t)}} \right)$ for identifying the best arms, without accounting for the transmit power.

Fig. 1 shows the evolution of the percentage of users with a successful transmission (PST), *i.e.* having $\Gamma_{k,a_{\text{best}}^{(k)}} \geq \Gamma^r$, in terms of the requested rate in Mbps, while Fig. 2 shows

the corresponding average transmit power per device. We can first note how the Enhanced-UCB algorithm outperforms the UCB in terms of the transmit power which is smaller for all values of the requested rate. However, Enhanced-UCB trades the probability of success for the transmit power and therefore presents a lower PST compared to UCB. Indeed, at a requested rate of 0.5 Mbps, Enhanced-UCB spares an average transmit power of 3.5 dBm, with a loss in PST of almost 10%. The RA method leads to a significantly higher power and a much lower PST when compared to Enhanced-UCB.

Moreover, when comparing the DCC setup to the ALL setup, one can see that both methods necessitate a very close transmit power and yield the same performance in terms of PST. This observation is valid for all values of the requested rate, while in previous works like [21] that compared the two setups in the uplink, a small loss in performance was generally observed in DCC. In fact, DCC reduces the number of involved APs per user, compared to ALL, and therefore the denominator of the SINR in (8). More specifically, the interference of some of the signals that have not been removed yet by SIC (corresponding to lower power levels on the same subband) on the signal of device k is reduced, which tends to increase the SINR. However, this gain in SINR is also counteracted by an increase in the transmit power of k, which can be seen when observing the denominator of (5) that decreases by DCC compared to ALL. The slight increase in the transmit power, which is noticeable in the small rate region of fig. 2, can sometimes lead to a reduction in the number of available arms for k (recall that arms that exceed the power budget are blocked by the system design). However, if the involved APs are well selected among the best ones that can efficiently serve the users, the removed ones by $\mathbf{D}_k$ should have a minor influence on the overall channel gain of the device k. As the required rate increases, it reaches a point where the number of valid arms in the sets $\mathcal{A}_k, k = 1, \cdots, K$, becomes limited. Thus, the number of collisions grows (since devices tend to choose the same arms) and the realized rates deteriorate rapidly, for both UCB and Enhanced-UCB, as well as the PST.

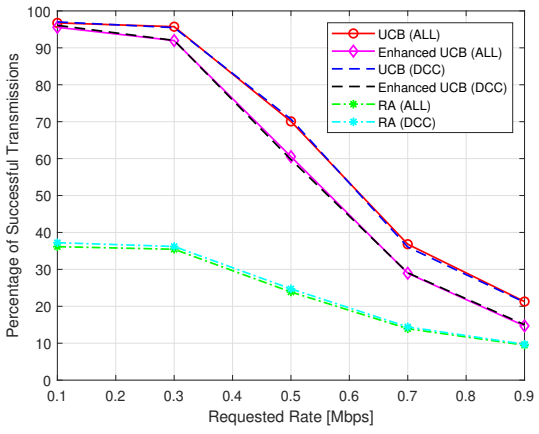

Fig. 1. PST in terms of the requested data rate

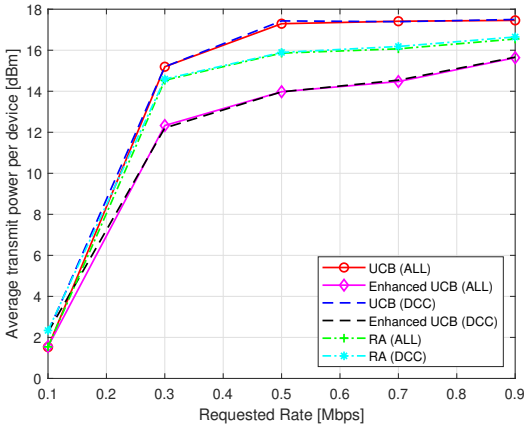

Fig. 2. Average transmit power per device in terms of the requested data rate

In Figs. (3) and (4), we study the convergence of the UCB and Enhanced-UCB algorithms by showing the evolution of the PST and the total transmit power (of all devices) for the different methods over the time horizon, with a target rate of 0.5 Mbps. The results show that the UCB-ALL and UCB-DCC techniques have the fastest convergence and reach a PST of 98% and 97%, respectively, after 50 timeslots. Enhanced-UCB-ALL and Enhanced-UCB-DCC come next in convergence and reach 94% and 93% after 60 timeslots, respectively. The RA scheme has the poorest PST which keeps fluctuating around 37%. Its total transmit power is much higher than that of Enhanced-UCB and close to that of UCB, evolving around 31.6 dBm, compared to 29 dBm and 32.2 dBm for Enhanced-UCB-DCC and UCB-DCC respectively.

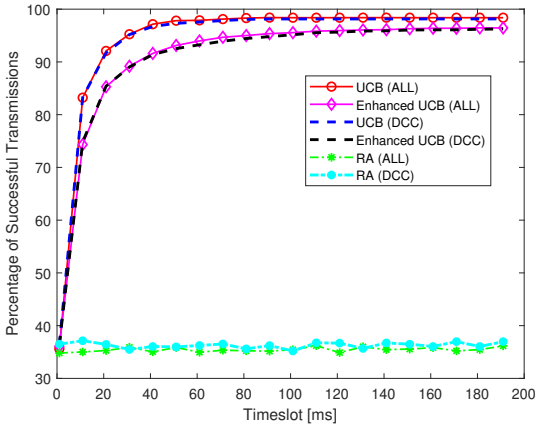

Fig. 3. PST in terms of the timeslot number

V. Conclusion

In this paper, the uncoordinated resource allocation problem in cell-free massive MIMO NOMA is solved for the first time using a reinforcement learning framework. In this framework, devices randomly deployed in the coverage area determine

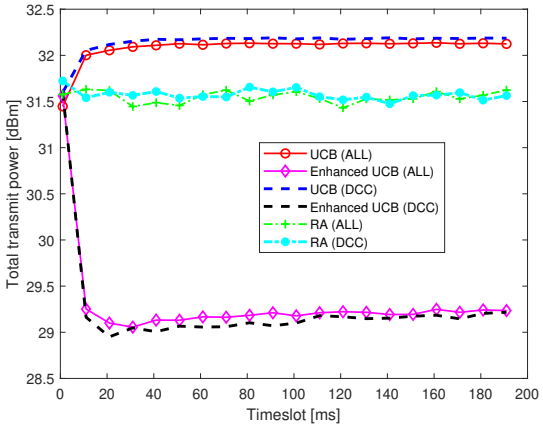

Fig. 4. Total transmit power in terms of the timeslot number

their subband and transmit power without any cooperation using a strategy based on the UCB algorithm. This method is applied in two cell-free configurations: one that serves devices through a well-chosen, pre-selected subset of APs, and another that uses the entire set of deployed APs. The results showed that the first scenario has a negligible loss in performance compared to the second in terms of the probability of success and the transmit power of the devices. It was also shown that, as in [19], integrating the transmit power into the decision metric allows devices to settle on arms that tend to spare their transmit power while slightly reducing their chances of meeting their QoS requirements. The current study was performed under the assumption of a centralized operation, where the CPU performs signal combining based on the received signals from the APs, which act as distributed RRHs. The study can be directly extended to the case of a distributed operation where the SIC is implemented at the level of more intelligent APs. Such an interesting extension of the current work can also include the influence of imperfect channel estimation.

REFERENCES

[1] G. Interdonato, E. Björnson, H. Quoc Ngo, P. Frenger, and E. G. Larsson, "Ubiquitous Cell-Free Massive MIMO Communications," *EURASIP Jour. on Wir. Commun. and Netw.*, vol. 2019, no. 1, pp. 1–13, 2019.

[2] Z. Chen and E. Björnson, "Channel Hardening and Favorable Propagation in Cell-Free Massive MIMO with Stochastic Geometry," *IEEE Trans. on Commun.*, vol. 66, no. 11, pp. 5205–5219, 2018.

[3] E. P. Simon, P. Laly, J. Farah, E. Tanghe, W. Joseph, and D. P. Gaillot, "Measurement of the V2I Channel in Cell-free Vehicular Networks with the Distributed MaMIMOSA Channel Sounder," in *2023 17th European Conf. on Antennas and Propagation (EuCAP)*, 2023.

[4] D. Löschenbrand, M. Hofer, L. Bernadó, S. Zelenbaba, and T. Zemen, "Towards Cell-Free Massive MIMO: A Measurement-Based Analysis," *IEEE Access*, vol. 10, pp. 89 232–89 247, 2022.

[5] T. Choi, M. Ito, I. Kanno, J. Gomez-Ponce, C. Bullard, T. Ohseki, K. Yamazaki, and A. F. Molisch, "Energy Efficiency of Uplink Cell-Free Massive MIMO With Transmit Power Control in Measured Propagation Channel," *IEEE Open Jour. of Cir. and Sys.*, vol. 2, pp. 792–804, 2021.

[6] T. Choi, P. Luo, A. Ramesh, and A. F. Molisch, "Co-Located vs Distributed vs Semi-Distributed MIMO: Measurement-Based Evaluation," in *54th Asilomar Conf. on Sig., Sys., and Computers*, 2020, pp. 836–841.

[7] M. Rahmani, M. Bashar, M. J. Dehghani, P. Xiao, R. Tafazolli, and M. Debbah, "Deep Reinforcement Learning-based Power Allocation in Uplink Cell-Free Massive MIMO," in *2022 IEEE Wireless Commun. and Networking Conf. (WCNC)*, 2022, pp. 459–464.

[8] Y. Zhang, J. Zhang, Y. Jin, S. Buzzi, and B. Ai, "Deep Learning-Based Power Control for Uplink Cell-Free Massive MIMO Systems," in *2021 IEEE Global Commun. Conference (GLOBECOM)*, 2021, pp. 1–6.

[9] M. Farooq, H. Q. Ngo, and L. N. Tran, "Mirror Prox Algorithm for Large-Scale Cell-Free Massive MIMO Uplink Power Control," *IEEE Commun. Letters*, vol. 26, no. 12, pp. 2994–2998, 2022.

[10] M. Guenach, A. A. Gorji, and A. Bourdoux, "Joint Power Control and Access Point Scheduling in Fronthaul-Constrained Uplink Cell-Free Massive MIMO Systems," *IEEE Trans. on Commun.*, vol. 69, no. 4, pp. 2709–2722, 2021.

[11] Y. Yuan, S. Wang, Y. Wu, H. V. Poor, Z. Ding, X. You, and L. Hanzo, "NOMA for Next-Generation Massive IoT: Performance Potential and Technology Directions," *IEEE Commun. Magazine*, vol. 59, no. 7, pp. 115–121, 2021.

[12] Y. Zhang, H. Cao, M. Zhou, and L. Yang, "Spectral Efficiency Maximization for Uplink Cell-Free Massive MIMO-NOMA Networks," in *2019 IEEE Int. Conf. on Commun. Workshops (ICC Workshops)*, 2019, pp. 1–6.

[13] T. K. Nguyen, H. H. Nguyen, and H. D. Tuan, "Max-Min QoS Power Control in Generalized Cell-Free Massive MIMO-NOMA With Optimal Backhaul Combining," *IEEE Trans. on Vehicular Tech.*, vol. 69, no. 10, pp. 10 949–10 964, 2020.

[14] M. Hua, W. Ni, H. Tian, and G. Nie, "Energy-Efficient Uplink Power Control in NOMA Enhanced Cell-Free Massive MIMO Networks," in *2021 IEEE/CIC Int. Conf. on Commun. in China (ICCC Workshops)*, 2021, pp. 7–12.

[15] Y. Zhang, H. Cao, M. Zhou, and L. Yang, "Spectral Efficiency Maximization for Uplink Cell-Free Massive MIMO-NOMA Networks," in *2019 IEEE Int. Conf. on Commun. Workshops (ICC Workshops)*, 2019, pp. 1–6.

[16] J. Zhang, X. Tao, H. Wu, N. Zhang, and X. Zhang, "Deep Reinforcement Learning for Throughput Improvement of the Uplink Grant-Free NOMA System," *IEEE Int. of Things Jour.*, vol. 7, no. 7, pp. 6369–6379, 2020.

[17] M. J. Youssef, V. V. Veeravalli, J. Farah, and C. Abdel Nour, "Stochastic Multi-Player Multi-Armed Bandits with Multiple Plays for Uncoordinated Spectrum Access," in *2020 IEEE 31st Int. Symp. on Pers., Indoor and Mobile Radio Commun. (PIMRC)*, Sept. 2020, pp. 1–7.

[18] M.-J. Youssef, V. V. Veeravalli, J. Farah, C. A. Nour, and C. Douillard, "Resource Allocation in NOMA-Based Self-Organizing Networks Using Stochastic Multi-Armed Bandits," *IEEE Trans. on Commun.*, vol. 69, no. 9, pp. 6003–6017, 2021.

[19] J. Doumit, M.-J. Youssef, C. A. Nour, J. Farah, and C. Douillard, "Resource Allocation in Full-Duplex Uncoordinated Communication Systems with NOMA," in *IEEE 32nd Annual Int. Symp. on Personal, Indoor and Mobile Radio Commun. (PIMRC)*, 2021, pp. 1104–1110.

[20] I. Bistritz and A. Leshem, "Distributed Multi-Player Bandits - a Game of Thrones Approach," in *Advances in Neural Inf. Process. Syst.*, vol. 31. Curran Associates, Inc., 2018, pp. 7222–7232.

[21] O. T. Demir, E. Björnson, and L. Sanguinetti, "Foundations of User-Centric Cell-Free Massive MIMO," *Foundations and Trends® in Signal Processing*, vol. 14, no. 3-4, pp. 162–472, 2021. [Online]. Available: http://dx.doi.org/10.1561/2000000109.

[22] S. Chen, J. Zhang, E. Björnson, J. Zhang, and B. Ai, "Structured Massive Access for Scalable Cell-Free Massive MIMO Systems," *IEEE Journal on Sel. Areas in Commun.*, vol. 39, no. 4, pp. 1086–1100, 2021.

[23] J. Farah, E. P. Simon, P. Laly, and G. Delbarre, "Efficient Combinations of NOMA with Distributed Antenna Systems based on Channel Measurements for Mitigating Jamming Attacks," *IEEE Systems Journal*, vol. 15, no. 2, pp. 2212–2221, 2020.

[24] J. Farah, J. Akiki, and E. P. Simon, "Energy-Efficient Techniques for Combating the Influence of Reactive Jamming using Non-Orthogonal Multiple Access and Distributed Antenna Systems," in *2019 Wireless Telecommun. Symposium (WTS)*. IEEE, 2019, pp. 1–7.

[25] J. Choi, "NOMA-Based Random Access With Multichannel ALOHA," *IEEE J. Sel. Areas in Commun.*, vol. 35, no. 12, pp. 2736–43, Oct. 2017.

[26] M. A. Adjif, O. Habachi, and J. P. Cances, "Joint Channel Selection and Power Control for NOMA: A Multi-Armed Bandit Approach," in *2019 IEEE Wireless Commun. and Netw. Conf. Workshop (WCNC)*, Marrakech, Morocco, Apr. 2019, pp. 1–6.